Published in final edited form as:
J Neurosci. 2012 May 30; 32(22): 7454–7465. doi:10.1523/JNEUROSCI.6379-11.2012.

Caspase-6 activity in a BACHD mouse modulates steady state levels of mutant huntingtin protein but is not necessary for production of a 586 amino acid proteolytic fragment

Juliette Gafni[1], **Theodora Papanikolaou**[1], **Francesco DeGiacomo**[1], **Jennifer Holcomb**[1], **Sylvia Chen**[1], **Liliana Menalled**[2], **Andrea Kudwa**[2], **Jon Fitzpatrick**[2], **Sam Miller**[2], **Sylvie Ramboz**[2], **Pasi I. Tuunanen**[3], **Kimmo K. Lehtimäki**[3], **X. William Yang**[4], **Larry Park**[5], **Seung Kwak**[5], **David Howland**[5], **Hyunsun Park**[5], and **Lisa M. Ellerby**[1]

[1]Buck Institute for Research on Aging, Novato, CA 94945

[2]Psychogenics Inc, Tarrytown, NY 10591

[3]Cerebricon Ltd., (Charles River Discovery Services), Kuopio, Finland 70210

[4]Center for Neurobehavioral Genetics, Semel Institute for Neuroscience and Human Behavior, Department of Psychiatry & Biobehavioral Sciences, Brain Research Institute, David Geffen School of Medicine at UCLA, Los Angeles, CA 90095

[5]CHDI Management/CHDI Foundation, Inc., Los Angeles, CA 90045

SUMMARY

Huntington's disease (HD) is caused by a mutation in the huntingtin (Htt) gene encoding an expansion of glutamine repeats at the N-terminus of the Htt protein. Proteolysis of Htt has been identified as a critical pathological event in HD models. In particular, it has been postulated that proteolysis of Htt at the putative caspase-6 cleavage site (at amino acid Asp-586) plays a critical role in disease progression and pathogenesis. However, whether caspase-6 is indeed the essential enzyme that cleaves Htt at this site *in vivo* has not been determined. To evaluate, we crossed the BACHD mouse model with a caspase-6 knockout mouse (*Casp6*−/−) Western blot and immunocytochemistry confirmed the lack of caspase-6 protein in *Casp6*−/− mice, regardless of HD genotype. We predicted the *Casp6*−/− mouse would have reduced levels of caspase-6 Htt fragments and increased levels of full-length Htt protein. In contrast, we found a significant reduction of full-length mutant Htt (mHtt) and fragments in the striatum of BACHD *Casp6*−/− mice. Importantly, we detected the presence of Htt fragments consistent with cleavage at amino acid Asp-586 of Htt in the BACHD *Casp6*−/− mouse, indicating that caspase-6 activity cannot fully account for the generation of the Htt 586 fragment *in vivo*. Our data are not consistent with the hypothesis that caspase-6 activity is critical in generating a potentially toxic 586 amino acid Htt fragment *in vivo*. However, our studies do suggest a role for caspase-6 activity in clearance pathways for mHtt protein.

INTRODUCTION

Huntington's disease (HD) is a dominantly inherited neurodegenerative disorder characterized by progressive decline of cognitive and motor function due to loss of striatal and cortical neurons. HD is caused by a mutation in the huntingtin (Htt) gene encoding a glutamine repeat (CAG expansion) at the N-terminus of Htt (HDCRG, 1993). A neuropathological hallmark of HD is the accumulation of N-terminal Htt fragments,

Correspondence: Lisa M. Ellerby, Ph.D., lellerby@buckinstitute.org.

suggesting that Htt proteolysis may be a critical event in pathogenesis (Goldberg et al., 1996; Davies et al., 1997; DiFiglia et al., 1997; Martindale et al., 1998; Gutekunst et al., 1999; Gafni and Ellerby, 2002; Gafni et al., 2004).

Htt is cleaved by multiple proteases, including aspartyl proteases, calpains, γ-secretase and caspases (Goldberg et al., 1996; Wellington et al., 1998; Gafni and Ellerby, 2002; Lunkes et al., 2002; Gafni et al., 2004; Kegel et al., 2010). Indeed Htt was the first neuronal protein identified as a caspase substrate (Goldberg et al., 1996) and studies have defined the Htt cleavage sites for caspase-3 at amino acids (aa) Asp-513 and Asp-552, for caspase-2 at aa Asp-552, and for caspase-6 at the IVLD aa Asp-586 site (Wellington et al., 1998; Wellington et al., 2000; Hermel et al., 2004). Caspase-6 binds to Htt and dominant-negative caspase-6 blocks HD striatal neuronal degeneration (Hermel et al., 2004). Further, the processed form of caspase-6 can be found activated in mouse and human HD striatum (Hermel et al., 2004; Graham et al., 2010). Proteolytic cleavage of Htt at the caspase-6 site at aa Asp-586 may be an important event in the pathogenesis of HD (Graham et al., 2006). Interestingly, in a YAC128 mouse model of HD, mutation of the potential caspase-6 cleavage site at Asp-586 (YAC128 C6R; note also mutated Asp-589 site) in mHtt did not recapitulate behavorial phenotypes or a number of key pathological changes apparent in YAC128 mice that do not carry that mutation (Graham et al., 2006). However, it is not clear whether these differences in YAC128 C6R transgenic mice are due to the ablation of the caspase-6 cleavage site, altered expression levels, or to structural changes within Htt caused by the mutations at Asp-586 and Asp-589. Furthermore, it remains to be tested whether caspase-6 is the protease responsible for cleavage of Htt at Asp-586 and whether it is required for disease progression *in vivo*.

Caspase-6 activation has been implicated in other neurological conditions and diseases; it is activated early in sporadic and familial forms of Alzheimer's disease (AD) with active caspase-6 localized to neuropil threads, neuritic plaques and neurofibrillary tangles (Guo et al., 2004; Albrecht et al., 2009). Caspase-6 activation in AD models leads to neuritic beading, axonal degeneration and eventually cell death, which can be prevented by incubation with caspase-6 inhibitors or dominant negative caspase-6 (Nikolaev et al., 2009; Sivananthan et al., 2010). Active caspase-6 and caspase-6-cleaved tau have also been observed in non-cognitively impaired aged individuals that have the lowest cognitive scores, suggesting that caspase-6 activation may be an early step in cognitive decline (Albrecht et al., 2007).

Since caspase-6 activation has been identified in a number of neurological conditions and may play an important role in HD pathogenesis, we crossed the well characterized BACHD mouse model (Gray et al., 2008; Menalled et al., 2009) with a caspase-6 knockout mouse (*Casp6*$^{-/-}$) to test whether caspase-6 deficiency would prohibit production of the putative caspase-6-derived aa586 Htt fragment and lead to altered levels of full-length mutant or wild-type Htt. In addition, limited measures were followed to track the effects of caspase-6 knockout on behavior and histopathology in the BACHD mouse. We found that, counter to expectations, the aa586 Htt fragment remained abundant in the BACHD *Casp6*$^{-/-}$ mice and, moreover, the amount of full-length mHtt was markedly decreased. We report preliminary findings that suggest clearance pathways in the BACHD *Casp6*$^{-/-}$ mouse brain may be invoked to clear full-length mHtt, including activation of other proteases, macroautophagy, a lysosomal quality control pathway or other ubiquitin-mediated protein degradation pathways.

MATERIALS AND METHODS

Caspase-6 Knockout Mouse

Knockouts of the mouse caspase-6 gene were made at Taconic-Xenogen in C57BL/6 mice using homologous recombination in mouse embryonic stem cells and subsequent blastocyst injection of the appropriate targeted ES cells to create the gene targeted mice. The RP23-35M15 BAC clone was used to generate the homology arms and the conditional knockout region for the gene targeting vector, as well as the southern probes to screen for targeted events. All recombinant plasmids were confirmed by restriction digestion and end-sequencing and all exons were sequence confirmed. The final vector was obtained by standard molecular cloning. 30 μg of the Not I-linearized final KO vector DNA was electroporated into ~10^7 C57BL/6 ES cells. The cells were selected with 200 μg/ml G418 and 192 ES clones were picked for screening. Based on this Southern analysis using the 5′ 3′ and neo probes, four clones were confirmed to be correctly targeted and to have a single neo insertion. Clones were injected to produce 30 male chimeras, which were bred with wildtype females to generate heterozygotes. Initial characterization of the *Casp6*−/− mice is reported (Uribe et al.).

Transgenic Mouse Model Expressing Htt145Q (1–586)

The RMCE ES cell line (derived from mouse strain C57BL/6-Gt(ROSA)26Sor tm596Arte was grown on a mitotically inactivated feeder layer comprised of mouse embryonic fibroblasts (MEF) in DMEM High Glucose medium containing 20% FBS (PAN) and 1200 u/mL Leukemia Inhibitory Factor (Millipore ESG 1107). For manipulation 2×10^5 ES cells were plated on 3.5 cm dishes in 2 ml medium. For transfection, 3 μl Fugene6 Reagent (Roche; Catalog No. 1 814 443) was mixed with 100 μl serum free medium (OptiMEM I with Glutamax I; Invitrogen; Catalog No. 51985-035) and incubated for 5 min at room temperature (RT). 100 μl of the Fugene/OptiMEM solution was added to the DNA mixture containing 2 μg circular vector and 2 μg CAGGS-Flp plasmid. This transfection complex was incubated for 20 min at RT and then added dropwise to the cells. From day 2 onwards the medium was replaced daily with medium containing 250 μg/mL G418 (Geneticin; Invitrogen; Catalog No. 10131-019). Seven days later single clones were isolated, expanded and analyzed by Southern blotting according to standard procedures. After administration of hormones, superovulated Balb/c females were mated with Balb/c males. Blastocysts were isolated from the uterus at dpc 3.5. For microinjection, blastocysts were placed in a drop of DMEM with 15% FCS under mineral oil. A flat tip, piezo actuated microinjection-pipette with an internal diameter of 12–15 μm was used to inject 10–15 targeted C57BL/6 N.tac ES cells into each blastocyst. After recovery, 8 injected blastocysts were transferred to each uterine horn of 2.5 days post coitum, pseudopregnant NMRI females. Chimerism was measured in chimeras (G0) by coat color contribution of ES cells to the Balb/c host (black/white). Highly chimeric mice were bred to strain C57BL/6 females. The C57BL/6 mating partners were non-mutant or mutant for the presence of a recombinase gene. Germline transmission was identified by the presence of black, strain C57BL/6, offspring (G1).

Hdh Knockdown Mice

3-month old Hdh KD mice (inducible knockdown of mouse Htt with shRNA) were fed 3000 ppm doxycycline pellets for 4 weeks and then sacrificed. Samples were analyzed for western analysis as described below.

Mouse Development and Behavioral Evaluation

Subjects—Experimental female mice used in this study were bred at Taconic by crossing BACHD mutant female mice (FVB/N) (Gray et al., 2008) with male caspase-6 knock out

mice (C57BL/6) generated by Taconic-Xenogen. Mice arrived at PsychoGenics around 11–14 weeks of age. Mice were handled on 2 consecutive days (1 min each day), then tail tattooed and chipped (Datamars, Switzerland) for identification purposes. Mice were housed in Optimice cages containing wood shavings, play tunnels, shredded paper, and plastic bones. Mice had free access to water and unaltered Purina 5001 food diet pellets. On the day of the experiment, mice were allowed to acclimate to the testing room for at least one hour prior to the beginning of the experiment. Mice were transported from the colony room to the experimental room in their home cages.

Body Weight and General Health—Mice were weighed weekly throughout the course of the experiment, and general health was monitored on a daily basis. At Psycogenics, all procedures were approved by the Institutional Animal and Use Committee of Psychogenics, Inc. (PHS OLAW animal welfare assurance number A4471-01), an AAALAC International accredited institution (Unit #001213). At the Buck Institute for Research on Aging, an AAALAC international accredited institution (Unit #001070), all procedures were approved by the Institutional Animal and Use Committee (A4213-01).

Rotarod—Mice were tested over 3 consecutive days. Each daily session included a training trial of 5 min at 4 RPM on the rotarod apparatus. One hour later, the animals were tested for 3 consecutive accelerating trials of 5 min with the speed changing from 0 to 40 RPM over 300 seconds and an inter-trial interval of at least 30 min. The latency to fall from the rod on each of the three testing trials was recorded. Mice remaining on the rod for more than 300 sec were removed and their time was scored as 300 sec. Animals were evaluated at 16, 20, 24, 37 and 51 weeks of age.

Open field—Activity chambers (Med Associates Inc, St Albans, VT; 27 × 27 × 20.3 cm) were equipped with infrared (IR) beams. Mice were placed in the center of the chamber and their behavior was recorded for 30 min. Quantitative analysis was performed on the following five dependent measures: total locomotion, locomotion in the center of the open field, rearing rate in the center, total rearing frequency and velocity. Animals were evaluated at 16, 20, 24, 37 and 51 weeks of age.

Data Analysis of Weight and Behavior—An alpha level of 0.05 was selected for all inferential statistics. The repeated measures analysis (age as dependent factor) was carried out with SAS (SAS Institute Inc.) using Mixed Effect Models. This approach is based on likelihood estimation, which is more robust to missing values than moment estimation. The models were fitted using the procedure PROC MIXED (Singer, 1998). The BACHD, BACHD *Casp6+/−* and BACHD *Casp6−/−* groups were compared to evaluate the effect of the caspase-6 deficiency on the BACHD mice. Factors for analyses included caspase-6 genotype and age.

MRI analysis of BACHD and BACHD Casp6−/− mice—Mice were perfused transcardially with heparinized 0.9% saline followed by 4% PFA. Brains were removed from the skull and left in 4 % PFA until measured by MRI. Before imaging, the brains were rinsed with saline and embedded in perfluoropolyether (FOMBLIN). T2-weighted MRI was performed with the use of a horizontal 7 T magnet with inner bore diameter of 160 mm (Magnex Scientific Ltd., Oxford, UK) equipped with actively shielded Magnex gradient set (maximum gradient strength 400 mT/m) interfaced to a Varian DirectDrive console (Varian Inc., Palo Alto, CA USA). Linear RF volume-coil was used for transmission and surface phased array coil for receiving (Rapid Biomedical GmbH, Rimpar, Germany). For determination of *ex vivo* total brain, striatal and cortical volumes, T2-weighted continuous multi-slice images covering the whole brain were acquired using fast spin-echo sequence

with TR = 4500 ms, ETL = 4, effective TE = 37.7 ms, matrix size = 512 × 256 (zeropadded to 512×512), FOV = 30*30 mm^2, slice thickness = 0.6 mm, number of slices = 21 and four averages. The acquired coronal images were analyzed for total brain, striatal and cortical volumes using in-house written analysis program run under MATLAB (The MathWorks Inc, Natick, MA USA) environment. All values are presented as mean ± Standard Error of Mean (SEM), and differences are considered to be statistically significant at the $p<0.05$ level. Statistical analysis was performed using StatsDirect statistical software (StatsDirect Ltd, Altrincham, UK). p-values were not corrected for multiple comparison.

Biochemical Analysis

Huntingtin Neoepitope Antibody Production—Antibodies specific for the C-terminal ends of Htt caspase cleavage product ending at amino acid 586 was prepared using the immunizing peptide KLH-CPSDSSEIVLD. Peptide sequences were injected into rabbits, antibody was purified to the injected peptide and a bridging peptide was used to remove antibodies reacting to full-length Htt (Open Biosystems, Huntsville, AL). Antibodies were affinity purified as previously described with minor modifications (Gervais et al., 1999; Wellington et al., 2002; Leyva et al.).

Western Blot Analysis—Half the cortex and striatum from 13- and 15-month old animals were lysed in Tissue Protein Extraction Reagent (TPER; Thermo Scientific, Rockford, IL) with protease inhibitors (Complete Mini, Roche Applied Science, Mannheim, Germany) and 1 μM epoxymycin at 10 ml/g. In some cases, phosphatase inhibitors (Phosphatase Inhibitor Cocktail Set II, Calbiochem, La Jolla, CA) and HDAC inhibitors (50 μM TSA, 30 μM sodium butyrate, 30 mM nicotinamide) were also included. Tissue was homogenized, sonicated and spun at 14,000g for 20 min. Supernatant and pellets were kept for analysis. Protein concentration was determined using a BCA assay (Pierce, Rockford, IL) and 40–60 μg of protein was run on a polyacrylamide gel and transferred to a 0.45 μm nitrocellulose (Whatman, Dassel, Germany) or 0.2 μm polyvinylidene difluoride (Pall Life Sciences, Pensacola, FL) membrane. Polyclonal primary antibodies used were: cleaved caspase-6 9761(1:75, Cell Signaling, Beverly, MA), procaspase-6 9762 (1:125, Cell Signaling), procaspase-3 9662 (1:200, Cell Signaling), cleaved caspase-3 9661S (1:100, Cell Signaling), cleaved caspase-7 9491S (1:100, Cell Signaling), procaspase-9 9504 (1:100, Cell Signaling), cleaved caspase-9 9509 (1:100, Cell Signaling), cleaved lamin A/C 2031s (1:50, Cell Signaling), neoHtt586 90000188 (1:50, CHDI), LC3 PM036 (1:1000, MBL, Woburn, MA), LC3 AP1802a (1:100, Abgent, San Diego, CA), ubiquitin UG9510 (1:250, ENZO, Farmingdale, NY) and β-actin 4967 (1:1000, Cell Signaling). Monoclonal antibodies used were: Htt 2166 (1:500, Millipore, Billerica, MA), Htt 5490 (1:250, Millipore), Htt 1574 (1:1000, Millipore), caspase-2 3507 (1:100, Millipore), procaspase-7 56063 (1:200, Santa Cruz Biotechnology), p62 610833 (1:1000, BD Transduction Laboratories, San Jose, CA), GAPDH 10R-G109A (1:1000, Fitzgerald, Acton, MA) and fodrin 1622 (1:500, Millipore). Immunoblots were developed with a peroxidase-conjugated secondary antibody and enhanced chemiluminescence. For positive controls, lysates were treated with caspase-6 (400 U, ENZO) for 2 h at 37°C. It should be noted that while both LC3 antibodies were made against the LC3B isoform, there is no evidence they are specific for this LC3 subtype (Zois et al., 2011). Densitometry was performed using ImageQuant TL v2005 software. Statistics was performed using GraphPad Prism version 4.0c. For ANOVA, Tukey's Multiple Comparison post hoc test was used.

Formic Acid Pellet Extraction—Pellets from lysing protocol were incubated with 1 ml 70% formic acid for 1 h with shaking and then spun at 14,000g for 20 min. 750 μl of supernatant was transferred to a new tube and formic acid evaporated in a vacuum dryer. Remaining solid was re-suspended in 50 μl resuspension buffer (1X NuPAGE LDS buffer

(Invitrogen, Carlsbad, CA), 2% SDS, 5 μM DTT), boiled for 10 min, sonicated for 5 min and re-boiled for 10 min. 20μl was spun down at 16,100g for 30 min and 15μl was loaded on a polyacrylamide gel. Proteins were transferred to 0.45 μm nitrocellulose membrane (Whatman) and blots were probed as specified in western analysis section.

Immunohistochemistry—Formalin-fixed female and male WT, BACHD and BACHD *Casp6*−/− mice were paraffin-embedded, sectioned and deparaffinized with xylene. For cleaved caspase-6, neoHtt586 and ubiquitin immunohistochemistry, antigen retrieval was carried out by microwaving sections in 10 mM Citrate buffer (pH 6.0) for 2 min at maximum power and then 20% power for an additional 5 min (cleaved caspase-6, neoHtt586) or 5 min at 40% power (ubiquitin). Sections were incubated overnight at 4°C with polyclonal cleaved caspase-6 antibody 9761 (1:100, Cell Signaling) and polyclonal ubiquitin antibody 1690 (1:1000, Millipore) and with polyclonal neoHtt586 antibody (2.5 μg/ml, CHDI) for 3 hr at 37°C. Biotinylated anti-rabbit IgG secondary antibody (6 μg/ml, Vector, Burlingame, CA) was incubated 1 hr at RT followed by signal amplification with avidin/biotin (VECTASTAIN Elite ABC Reagent, Vector) and diaminobenzedine (DAB Peroxidase Substrate Kit, Vector) visualization. Mayer's Hematoxylin (American MasterTech, Lodi, CA) was used as a counterstain.

For LC3 immunohistochemistry a variation of Osmond et al. (2006) was performed. Briefly, following deparaffinization and rehydration, samples were formic acid treated 2 × 10 min and then incubated in 1% sodium borohydride for 20 min. Tissue was permeabilized with 0.4% Triton-100 and then polyclonal LC3 (PM036 antibody, 1:10,000, MBL) was applied overnight at 4°C. Biotinylated anti-rabbit IgG (6 μg/ml, Vector) was incubated for 1.5 h at RT followed by avidin/biotin (1:400, VECTASTAIN Elite ABC Kit, Vector) application for 1 h at RT. Amplification of signal was performed by incubating in biotinylated tyramine for 10 min followed by repeating aviden/biotin incubation. Sections were developed with diaminobenzedine and counterstained with hematoxylin as described above.

For ubiquitin/Htt double immunofluorescence, antigen retrieval was performed in 10 mM citrate buffer by microwaving for 5 min at 40% power. Chicken anti-mouse IgG (2 μg/ml, Aves Labs, Tigard, OR) was added to block buffer and slides were incubated with polyclonal ubiquitin 1690 (1:100, Millipore) and monoclonal Htt 2166 (1:200, Millipore) overnight at 4°C. For p62/acetyl-Htt-Lys-444 double immunofluorescence, antigen retrieval was performed in 10 mM citrate buffer by microwaving for 10 min at 40% power and then sequentially incubated with polyclonal p62 (1:100, Progen, Heidelberg, Germany) and polyclonal acetyl-Htt-Lys-444 (1:50, Open Biosystems) for 3 hr at RT. After primary antibody incubation, secondary antibodies Alexa Fluor 488 or 555 goat anti-rabbit IgG, Alexa Fluor 555 goat anti-guinea pig IgG and/or Alexa Fluor 488 goat anti-mouse IgG (1:500, Invitrogen) were incubated for 1 h at RT followed by coverslipping with Prolong Gold containing DAPI (Invitrogen). The custom Htt acetylation antibody (acetyl-Htt-Lys-444, Open Biosystems) was produced by injecting synthesized peptide corresponding to Htt acetylated at lysine 444 into rabbits. At day 58, bleeds were collected and serum was separated from plasma and tested for signal by western blot analysis. Those with positive results were purified by affinity binding and stored for use (Cong et al., 2011).

For polyclonal aggregate antibody S830 single labeling (7.0 μg/ml, gift of the A. Osmond and G. Bates), antigen retrieval was performed by microwaving 4 × 5 min at 40% power in 10 mM citrate buffer and then treating with Proteinase K (20 μg/ml; Eastman Kodak Scientific) for 10 min at 37°C. Duplicate photos were taken from the same area of cortex and striatum at identical magnification and exposure settings. Aggregates and DAPI stained nuclei were quantified using Imaris X64 7.3.0 software. Aggregate number was normalized to the number of DAPI stained nuclei in the field.

Primary Cultures and Immunocytochemistry—E17–18 embryos were obtained from timed pregnant C57BL/6 and *Casp6*−/− mice. Briefly, striatal tissue was dissociated with scalpels, trypsinized for 5–8 min (0.25% Trypsin/EDTA, Cellgro, Manassas, VA) and triturated with a pipette 15–20 times. After centrifugation and rinsing with fresh 20% FBS in DMEM (Cellgro), cells were resuspended in Neurobasal complete media (Neurobasal A media, 1 mM Glutamax, 2% B27 and 1% penicillin/streptomycin (Invitrogen)) and filtered through a 70 μm nylon strainer. Cells were plated on 8-chamber, poly-D-lysine coated slides (Beckton Dickenson Franklin Lakes, NJ) at 400,000 cells/chamber in Neurobasal complete media supplemented with 1% FBS. After 72 hrs, cells were fixed with 4% paraformaldehyde in PBS for 20 min and permeabilized in 0.1–0.5% Triton in TBS for 15 min RT. Cells were incubated in polyclonal cleaved caspase-6 9761 (1:50, Cell Signaling) and monoclonal MAP2 M4403 (1:500, Sigma) overnight at 4°C. Fluorescent secondary antibodies Alexa Fluor 488 goat anti-rabbit IgG and Alexa Fluor 555 goat anti-mouse IgG (1:500, Invitrogen) were incubated for 1 h at RT and slides were coverslipped with Prolong Gold containing DAPI (Invitrogen).

Quantitative RT-PCR for Htt and Caspase-6 cDNAs—Total RNA from 12-month old C57BL/6 and *Casp6*−/− striatum was extracted using the miRNeasy Mini Kit (Qiagen, Valencia, CA) and homogenized by triturating with a 27 ½ gauge needle. cDNAs were made from 1.0 μg of RNA samples using Message Sensor RT kit (Ambion, Austin, TX) and then 75 ng of each cDNA was pre-amplified for 14 cycles using Applied Biosystem's (Foster City, CA) TaqMan PreAmp master mix and protocol to generate PCR templates. Forward and reverse primers for the three genes of interest (Htt, caspase-6 and β-actin) were designed using Roche's Universal Probe Library Assay Design Center and ordered from Operon (Huntsville, AL) and Sigma (St. Louis MO). For Htt, nucleotides 4944–5004, 9301–9367 and 4822–4890 were amplified. For caspase-6, nucleotides 33–133, 150–262 and 264–373 were amplified and results were averaged. The real-time quantitative PCR was performed with SYBRGreen (Applied Biosystems) on a Light Cycler 480 (Roche) according to manufacturer's instructions.

RESULTS

Caspase-6 is Activated in BACHD Mouse Brains

Caspase-6 is activated during aging and in postmortem HD and AD brain (Hermel et al., 2004; Graham et al., 2006; Albrecht et al., 2007). Further, characterization of the YAC128 mouse model of HD shows an age-dependent increase in caspase-6 activation (Graham et al., 2010). To confirm that caspase-6 is activated in BACHD mice, sections of WT and BACHD were immunostained with an antibody that detects active mouse caspase-6 at 9 months of age (n= 3). As predicted, WT mice at this age had detectable active caspase-6 in the striatal medium-spiny and cortical neurons by 9 months (Fig. 1A). The staining was dendritic and nuclear in localization. Consistent with previous work (Graham et al., 2010), the BACHD mouse displayed an increase in activation of caspase-6 when compared to WT mice both in the striatum and cortex (Fig. 1A). This was also confirmed by western blot analysis of these mice at 9 months of age with a 2.5-fold increase in active caspase-6 in the striatum (Fig. 1B).

Caspase-6 Knockout Abolishes the Expression of Caspase-6

In order to evaluate the role of caspase-6 in HD, we generated caspase-6 knockout mice using homologous recombination at Taconic-Xenogen. A BAC clone was utilized for generating the homology arm and targeting vector. The targeting vector (Fig. 2A) was electroporated into C57BL/6 ES cells and Southern analysis identified several clones utilized for microinjection to generate caspase-6 knockout mice. The *Casp6*−/− mice were

viable, bred well and had no obvious phenotype. To determine if caspase-6 levels were eliminated in the caspase-6 knockout mice, we carried out western blot analysis (Fig. 2B) and evaluated active caspase-6 immunoreactivity in primary striatal neurons derived from WT and *Casp6−/−* mice (Fig. 2C). Western blotting and immunocytochemistry demonstrated the elimination of procaspase-6 and active caspase-6, respectively.

Having established that the *Casp6−/−* mice lacked the targeted protein, we crossed BACHD with *Casp6−/−* mice. Western blot analysis of WT (littermate controls), BACHD and BACHD *Casp6−/−* at 13-months of age demonstrates the elimination of the inactive p32 proform of caspase-6 in both the striatum and cortex of BACHD *Casp6−/−* mice (Fig. 2D, E). Further, we observed a decrease in the proform of caspase-6 when comparing WT to BACHD mice in both the striatum and cortex (Fig. 2D, E) consistent with the activation of this enzyme in HD mouse models. As expected, cleavage of the caspase-6 substrate, lamin C, is eliminated in the BACHD *Casp6−/−* mice suggesting a functional knockout of caspase-6 (Fig. 2D).

BACHD Caspase-6 Knockout has Reduced Htt Levels in the Striatum

Given that Htt is predicted to be a substrate of caspase-6, we examined whether the proteolysis of Htt was altered in the absence of caspase-6 both in the striatum (Fig. 3) and cortex (data not shown) of WT, *Casp6−/−*, BACHD and BACHD *Casp6−/−*. We predicted that blocking caspase-6 cleavage would reduce the level of fragmentation of Htt and preserve full-length Htt protein. As shown in Fig. 3A, we found the levels of full-length Htt reduced in the BACHD *Casp6−/−* striatum when compared to BACHD mice. Further, there was a two-fold decrease in the level of polyQ expanded Htt fragments in the BACHD *Casp6−/−* when compared to BACHD mice (Fig. 3B) as detected by the 1C2 antibody. The change in levels of full-length Htt can be largely attributed to a decrease in the level of polyQ-expanded Htt as shown in Fig. 3C. Indeed, the levels of Htt with 97 glutamine repeats was reduced four-fold in the BACHD *Casp6−/−* when compared to BACHD mice (Fig. 3C). The wild-type levels of full-length Htt appear reduced as well but the change in expression between BACHD and BACHD *Casp6−/−* did not reach statistical significance (Fig. 3C). When expanded full-length Htt levels were quantified relative to wild-type we observed a two-fold decrease in the mutant:normal Htt ratio in BACHD *Casp6−/−* relative to BACHD mice (data now shown; n=3, t-test, **, $p<0.01$). We also evaluated the proteolysis of Htt in the cortex and found similar but less robust changes in the level of expression of Htt in BACHD *Casp6−/−* when compared to BACHD mice (data not shown). In the cortex, we also observed a significant 1.5-fold decrease in expanded full-length Htt levels relative to wild-type levels in the BACHD *Casp6−/−* (data not shown; n=3, t=test, *, $p<0.05$). A relatively trivial explanation for the changes in protein levels could be that the knockout of caspase-6 altered the levels of Htt mRNA. However, as shown in Fig. 3D, the levels of mRNA for Htt were not altered in the *Casp6−/−* mice when compared to WT. As a control, the levels of mRNA for caspase-6 were measured and as expected are absent in the *Casp6−/−* mice (Fig. 3D).

Huntingtin Aggregates are Reduced in BACHD Caspase-6 Knockout Mice

Htt aggregates are associated with disease pathology in both human HD patients and HD animal models (Lee and Kim, 2006; Hoffner et al., 2007). While some studies identify Htt aggregates as toxic, others suggest that they are protective in nature (Hodgson et al., 1999; Sanchez et al., 2003; Zhang et al., 2008; Richards et al., 2011). We were interested in determining levels of Htt aggregates in BACHD *Casp6−/−* mice, relative to BACHD mice, not only because of their relationship to disease progression, but also to determine whether the decrease in soluble full-length Htt in BACHD *Casp6−/−* mice is due to re-localization of Htt to inclusion bodies. Thus, we performed immunohistochemistry using a specific

antibody that detects aggregated Htt, S830 (Steffan et al., 2000). We found Htt aggregates were dramatically decreased in the striatum and cortex of BACHD *Casp6*−/− mice relative to BACHD mice, with a four-fold decrease in the striatum and an eight-fold decrease in the cortex (Fig. 4A, B). Virtually no staining was observed in WT mice showing the specificity of the antibody (Fig. 4A,B).

BACHD Caspase-6 Knockout Mice do not Show a Reduction in the Proteolysis of Htt at aa586

Next, we evaluated whether caspase-6 is the protease solely responsible for the cleavage of Htt at aa586. We found that there was no change in the cleavage products for both wild-type and mutant Htt in WT, BACHD, and BACHD *Casp6*−/− cortex and striatum that migrated at a molecular weight similar in size to the aa586 Htt cleavage product (Fig. 6A–C).

In order to detect the aa586 Htt cleavage products we generated a series of neo-epitope rabbit antibodies to the site; the polyclonal serum only detects the aa586 Htt cleavage product and not others (Fig. 5A,B). The purified polyclonal neoHtt antibody appears to be selective to cleaved Htt since in a HD transgenic mouse over-expressing the Htt586 fragment, the immunoreactivity is greatly increased relative to WT and in an inducible Htt RNAi knockdown model (*SFN2009* L. B. MENALLED et al.) the signal decreases with the reduction of mouse Htt (Fig. 5B,C). When we evaluated these antibodies using the soluble lysates described in Fig. 6A–C we were not able to detect Htt immunoreactive to neoHtt586 in older animals. However, when we formic acid extracted proteins from the pellets, we were able to detect both wild-type and expanded Htt reactive to the neoHtt586 antibody (Fig. 6D,E) suggesting that the product is insoluble. The cleavage product was not reduced in the BACHD *Casp6*−/− striatum suggesting it is possible another protease cleaves Htt at this site. In addition, performance of caspase activity assays on striatal tissue and cultures using the caspase-6 substrate, VEID, showed an increase in VEIDase activity in *Casp6*−/− lysates, again suggesting another protease may be involved in Htt586 production (data not shown). It should be noted that VEID is also a caspase-3 substrate, which may be a reason for the increase in VEIDase activity observed (McStay et al., 2008).

To further characterize whether Htt is cleaved at amino acid 586 *in vivo*, we carried out immunohistochemistry of WT, BACHD and BACHD *Casp6*−/− in cortex and striatum using neoHtt586. We found increased immunoreactivity of neoHtt586 in the BACHD compared to WT (n=3, Fig. 6F). We detected decreased immunoreactivity of neoHtt586 in the BACHD *Casp6*−/− mouse brain, which may be related to the clearance of Htt described above.

Characterization of Behavioral Phenotype of BACHD Caspase-6 Knockout

Behavioral Evaluation and General Health—Systematic behavioral analysis has previously been used to phenotype numerous mouse models of HD, including the BACHD mice (Menalled et al., 2009). Studies using two different strains of BACHD mice showed impaired rotarod performance, hypoactivity in the open field test and an increased body weight compared to WT from an early age (Gray et al., 2008; Menalled et al., 2009). In order to determine if knocking out caspase-6 protects against health and behavioral deficits, body weight, brain volume and motor performance were measured in BACHD and BACHD *Casp6*−/− animals. BACHD *Casp6*+/−mice were included to study the effects of gene dosage.

Body Weight—In order to determine if there were changes in body weight, mice were weighed weekly up to 51 weeks of age. The body weight of the BACHD mice examined in this study was comparable to previous findings (Gray et al., 2008; Menalled et al., 2009). BACHD *Casp6*−/− weighed significantly less than BACHD mice at 16 weeks and from 19

to 40 and from 42 to 45 weeks of age (Fig. 7A, caspase-6 knockout genotype × Age interaction, $F(80,915)=1.51$, $p<0.01$; caspase-6 knockout genotype main effect, $F(2,23)=4.44$, $p<0.05$; Age main effect, $F(40,915)=11.53$, $p<0.0001$, simple main effects, $ps<0.05$). BACHD *Casp6*$^{-/-}$ were also found to be significantly smaller than BACHD *Casp6*$^{+/-}$at 51 weeks of age ($ps<0.05$) and BACHD *Casp6*$^{+/-}$were significantly smaller than BACHD mice from 48 to 51 weeks of age ($ps<0.05$) (Fig. 7A).

Rotarod and Open Field Test—Next, we evaluated the motor performance of the BACHD relative to BACHD *Casp6*$^{-/-}$ mice at 16, 20, 24, 37 and 51 weeks of age using conditions previously published (Menalled et al., 2009). The performance of the BACHD mice examined in this study is comparable to previous findings (Gray et al., 2008; Menalled et al., 2009). BACHD mice show rotarod deficits as early as 16 weeks of age and the deficit is progressive with age. As shown in Fig. 7B, knockout of caspase-6 resulted in only a modest improvement in rotarod performance with both BACHD *Casp6*$^{-/-}$ and BACHD *Casp6*$^{+/-}$showing an increase in latency to fall relative to BACHD mice at all time points tested (caspase-6 knockout genotype main effect, $F(2,23)=7.40$, $p<0.01$; Age main effect, $F(4,92)=12.02$, $p<0.0001$; caspase-6 knockout genotype × age interaction, $F(8,92)=0.89$, $p=0.5253$). Behavior in the open field was also assessed at 16, 20, 24, 37 and 51 weeks of age. When the total locomotion, locomotion in the center of the open field, rearing rate in the center, total rearing frequency and average velocity were evaluated, no behavioral rescue was observed in the BACHD *Casp6*$^{-/-}$ mice relative to BACHD in any of the aforementioned test parameters (data not shown).

MRI analysis of WT, BACHD and BACHD *Casp6*$^{-/-}$—In order to assess whether there are changes in tissue volume, MRI analyses of WT, BACHD, BACHD *Casp6*$^{+/-}$and BACHD *Casp6*$^{-/-}$ were performed. While BACHD mice had smaller whole brain volume than WT at 16 months of age, they had a smaller striatal volume at 6, 12, and 16 months of age (Fig. 7C, E). In contrast, there were no differences in cerebellar volume between BACHD and WT mice at any age (data not shown). When BACHD, BACHD *Casp6*$^{+/-}$and BACHD *Casp6*$^{-/-}$ whole brain and striatal volumes were compared at 13 months of age, no significant differences were observed (Fig. 7D,F). This suggests that knockout of caspase-6 does not have a profound effect on brain neuropathology.

Analysis of Potential mHtt Clearance Pathways in BAC *Casp6*$^{-/-}$ Mice—Given the observation that Htt levels are altered in the BAC *Casp6*$^{-/-}$ mice we decided to evaluate known pathways involved in cleaving Htt or clearing the protein. It is well established for a number of caspase knockout mice that compensatory up-regulation and activation of other family members can contribute to the lack of phenotype in these models (Zheng et al., 2000; MacFarlane, 2001). To explore the potential compensatory pathways in the *Casp6*$^{-/-}$ mice we evaluated the expression of caspase-2, caspase-3, caspase-7, caspase-8, caspase-9 and caspase-12. We did not detect any measurable changes in the striatum, but did detect a significant increase in procaspase-3 in the BACHD *Casp6*$^{-/-}$ cortex when compared to BACHD cortex (Fig. 8, data not shown). We subsequently looked at cleaved caspase-2, caspase-3, caspase-7 and caspase-9 levels in both the striatum and cortex and did not observe any significant differences (data not shown). DEVD (caspase-3/7 substrate), VEID (caspase-3/6 substrate) and IETD (caspase-3/6/8/10 substrate) substrate cleavage in cortical and striatal lysates also was not significantly different (data not shown). These results suggest it is unlikely that the clearance of Htt observed in BACHD *Casp6*$^{-/-}$ is due to activation of other caspase family members.

To investigate other possible mechanisms responsible for the reduction in soluble mHtt and aggregates in the BACHD *Casp6*$^{-/-}$ mice, we measured the expression of LC3 and p62, proteins known to be involved in macroautophagy, as well as the acetylated form of Htt at

Lys-444, which has been recently shown to target mHtt to the autophagosome (Jeong et al., 2009). In addition, we analyzed protein ubiquitination, which is involved in the UPS clearance pathway.

We found that the LC3 levels are increased and localization is more concentrated to the cortical neuropil in BACHD *Casp6*−/− when compared to BACHD and WT mice (Fig. 9A, B). p62 levels were evaluated and may be decreased in BACHD *Casp6*−/− cortex relative to BACHD (Fig. 9C) (2.2-fold decrease; n=3–5, t-test, p=0.055). Since clearance of Htt has been shown to be regulated by acetylation at K444 in Htt (Jeong et al., 2009) and is critical for autophagy–regulated clearance mechanisms, we used double immunofluorescence of 13-month old BAC *Casp6*−/− cortex to show a cytosolic co-localization of acetylated Htt and p62 (Fig. 9D).

Ubiquitinated proteins often build up in HD mouse models and so, given the enhanced clearance of the Htt protein in the BACHD *Casp6*−/− mice, we analyzed ubiquitin and Htt distribution in the cortex of BAC *Casp6*−/− mice. We observed an overall decrease in ubiquitin staining in BAC *Casp6*−/− mice (Fig. 10A) and redistribution of ubiquitin staining from the nucleus in the BACHD mice to perinuclear localization in the BACHD *Casp6*−/− mice (Fig. 10B). We also observed an increased co-localization of Htt with ubiquitin in the BACHD *Casp6*−/− when compared to BACHD mice (Fig. 10C).

DISCUSSION

HD is caused by a mutation encoding a polyglutamine expansion at the N-terminus of Htt protein. It has been postulated that proteolytic processing of Htt leads to toxic fragments that drive disease progression, so the enzymes involved are potential therapeutic targets for HD. Previously, mice expressing mHtt that is not cleaved by caspase-6 but is cleaved by caspase-3 were shown to have normal neuronal function and were not susceptible to neurodegeneration (Graham et al., 2006). We therefore investigated whether the putative protease responsible for cleavage of Htt at Asp-586 was disease-modifying *in vivo*. Specifically, we crossed BACHD mice with *Casp6*−/− mice.

Previously, caspase-6 was suggested to be the key protease that cleaves Htt at aa586 (Graham et al., 2006), and so a homozygous caspase-6 knockout would be predicted to eliminate production of this Htt fragment. While we found that knocking out caspase-6 reduced expanded full-length Htt levels and overall Htt fragment levels, surprisingly it did not eliminate production of the aa586 Htt cleavage product. Interestingly, the YAC128 C6R mouse that showed full neurological rescue (Graham et al., 2006) was mutated at both the aa586 and aa589 sites, suggesting that either cleavage site may be involved in the phenotypic rescue. Alternatively, like the secretase pathways where mutation of the amyloid precursor protein site changes activity of the secretases, the rescue of YAC128 C6R could be due to altered protease activity (Golde et al., 2011). Analysis of a conditional caspase-6 knockout crossed to a HD mouse models is required to eliminate the possibility of compensatory pathways explaining our results. Further experiments will need to be conducted to confirm the cleavage site and key protease involved in Htt fragmentation.

No HD-like phenotypic abnormalities have been reported in the YAC128C6R mouse model (Graham et al., 2006) where a YAC128 mHtt transgene harboring the caspase-6 motif mutations (aa586 and aa589) was introduced into the mouse by transgenesis. Given the hypothesis that absence of caspase-6 cleavage at the mutated site in the YAC128 Htt protein leads to mice lacking an HD phenotype, we sought to independently investigate the effects of caspase-6 ablation on the general health, motor, and MRI phenotypes of the BACHD mouse model. BACHD *Casp6*−/− mice showed significant improvement in rotarod motor

performance compared to BACHD mice. The reduction in both soluble and insoluble mHtt aggregates may be responsible for this motor improvement, since reduction in expanded Htt levels has been shown to have a protective effect in HD (Ravikumar et al., 2002; Sanchez et al., 2003; Ravikumar et al., 2004). However, it should be noted that recent studies show that body weight can in part modulate rotarod performance in the BACHD line (unpublished data), making it possible that the improvement in rotarod performance in BACHD *Casp6*−/− mice is at least partly due to their reduced body weight. Interestingly, the reduced body weight in BACHD *Casp6*−/− and BACHD *Casp6*+/−animals may be a consequence of the unexpected reduction of full-length expanded Htt since it is known that full-length Htt levels in YAC128 mice can modulate body weight (Van Raamsdonk et al., 2006).

We have previously found that body weight also modulates the open field performance of mice, with smaller mice tending to present higher locomotor and rearing activity (unpublished data). Consequently the lack of effects of the caspase-6 knockout on locomotor and rearing activity exhibited by experimental mice in the open field task might be considered surprising given that they are significantly smaller than their WT counterparts. It is possible, however, that the knockout of caspase-6, independent of the BACHD genotype, induces a reduction of locomotor activity that is then masked by weight-related increases in activity; this possibility should be further investigated in the *Casp6*−/− mouse.

Our data do not support a neuroprotective effect of eliminating caspase-6 activity on mHTT-mediated whole brain and striatal atrophy, as measured in the BACHD mouse. Although these atrophies are modest in the BACHD mice we have no evidence that caspase-6 knock out prevents such changes.

A surprising finding of this study is the decrease in expanded full-length mHtt and mHtt fragments. We present preliminary evidence that soluble mHtt lowering and loss of mHtt aggregates may be modulated through enhanced protein clearance pathways in BACHD *Casp6*−/− mice. Interestingly, it has recently been shown that beclin, p62 and hAtg3 - each involved in autophagy - are substrates for caspase-6 cleavage (Norman et al., 2010). This connection between caspase-6 and protein clearance pathways led us to hypothesize that the *Casp6*−/− mice might exhibit altered levels of autophagy or ubiquitin proteasome system (UPS) activation. Our immunohistochemical analyses of BACHD *Casp6*−/− brain tissue suggests increased LC3 expression, with a redistribution in cortical neurons, as well as a decrease in p62 is consistent with the hypothesis that caspase-6 may be modulating autophagic clearance of mHtt. Furthermore, in cortical neurons of BACHD *Casp6*−/− mice we found evidence for increased association of p62 and K444-acetylated Htt relative to BACHD mice; the latter is a substrate for autophagy-mediated clearance (Jeong et al., 2009), and our results suggest it is altered in the homozygote *Casp6*−/− mice. Further work is required for a detailed understanding of the specific mechanisms engaged in the BACHD *Casp6*−/− mice that lead to lower levels of soluble mHtt and insoluble inclusion bodies. Autophagy would seem a viable candidate but our data showing a redistribution of ubiquitin staining and co-localization of Htt and ubiquitin in BAC *Casp6*−/− mouse brain raises the possibility that the UPS may be involved.

In summary, we show that elimination of caspase-6 protein and activity in the BACHD mouse model does not prevent the production of a 586 amino acid Htt proteolytic fragment in the brain. This data suggests that generation of this fragment *in vivo* is not due exclusively to caspase-6 activity and raises serious concerns about pursuing caspase-6 as a therapeutic target for HD in the context of the proteolytic fragment hypothesis. Studies using the HdhQ150 knockin model (Lin et al., 2001) crossed to the *Casp6*−/− mice saw no change in the general pattern of Htt fragmentation or level of the Htt586 product further supporting this conclusion (G. P. Bates, personal communication). Further investigation into cleavage

of Htt at the aa586 and aa589 sites is required to verify the key cleavage site, identify the protease responsible, and explore whether protease inhibition is a viable therapeutic strategy. An siRNA screen monitoring Htt586 or Htt589 cleavage levels as the endpoint may be an unbiased way to identify other potential proteases involved in this pathway. Future work directed at dissecting the role of caspase-6 in HD may require the use of conditional knockdown strategies to resolve the contributions of clearance pathways and Htt proteolysis.

Acknowledgments

This research was supported by grants from NIH: NS40251 (LME) and CHDI (LME). Neo Htt epitope antibodies and the Htt acetylation antibody were produced in collaboration with Jacqueline Duke and Matt Baker at OpenBiosystems. We thank both of them for their expert advice and help. Many thanks to Richard Mushlin for the statistical support and to Judy Watson-Johnson and Melinda Ruiz at Pysychogenics, Inc. for their technical assistance. We thank Gill Bates for the S829 and S830 Htt antibodies. We thank Dr. Osmond for protocols for immunostaining.

References

Albrecht S, Bogdanovic N, Ghetti B, Winblad B, LeBlanc AC. Caspase-6 activation in familial alzheimer disease brains carrying amyloid precursor protein or presenilin i or presenilin II mutations. Journal of neuropathology and experimental neurology. 2009; 68:1282–1293. [PubMed: 19915487]

Albrecht S, Bourdeau M, Bennett D, Mufson EJ, Bhattacharjee M, LeBlanc AC. Activation of caspase-6 in aging and mild cognitive impairment. The American journal of pathology. 2007; 170:1200–1209. [PubMed: 17392160]

Cong X, Held JM, DeGiacomo F, Bonner A, Chen JM, Schilling B, Czerwieniec GA, Gibson BW, Ellerby LM. Mass spectrometric identification of novel lysine acetylation sites in huntingtin. Mol Cell Proteomics. 2011; 10:M111 009829. [PubMed: 21685499]

Davies SW, Turmaine M, Cozens BA, DiFiglia M, Sharp AH, Ross CA, Scherzinger E, Wanker EE, Mangiarini L, Bates GP. Formation of neuronal intranuclear inclusions underlies the neurological dysfunction in mice transgenic for the HD mutation. Cell. 1997; 90:537–548. [PubMed: 9267033]

DiFiglia M, Sapp E, Chase KO, Davies SW, Bates GP, Vonsattel JP, Aronin N. Aggregation of huntingtin in neuronal intranuclear inclusions and dystrophic neurites in brain. Science. 1997; 277:1990–1993. [PubMed: 9302293]

Gafni J, Ellerby LM. Calpain activation in Huntington's disease. J Neurosci. 2002; 22:4842–4849. [PubMed: 12077181]

Gafni J, Hermel E, Young JE, Wellington CL, Hayden MR, Ellerby LM. Inhibition of calpain cleavage of huntingtin reduces toxicity: accumulation of calpain/caspase fragments in the nucleus. The Journal of biological chemistry. 2004; 279:20211–20220. [PubMed: 14981075]

Gervais FG, Xu D, Robertson GS, Vaillancourt JP, Zhu Y, Huang J, LeBlanc A, Smith D, Rigby M, Shearman MS, Clarke EE, Zheng H, Van Der Ploeg LH, Ruffolo SC, Thornberry NA, Xanthoudakis S, Zamboni RJ, Roy S, Nicholson DW. Involvement of caspases in proteolytic cleavage of Alzheimer's amyloid-beta precursor protein and amyloidogenic A beta peptide formation. Cell. 1999; 97:395–406. [PubMed: 10319819]

Goldberg YP, Nicholson DW, Rasper DM, Kalchman MA, Koide HB, Graham RK, Bromm M, Kazemi-Esfarjani P, Thornberry NA, et al. Cleavage of huntingtin by apopain, a proapoptotic cysteine protease, is modulated by the polyglutamine tract. Nature Genetics. 1996; 13:442–449. [PubMed: 8696339]

Golde TE, Schneider LS, Koo EH. Anti-abeta therapeutics in Alzheimer's disease: the need for a paradigm shift. Neuron. 2011; 69:203–213. [PubMed: 21262461]

Graham RK, Deng Y, Carroll J, Vaid K, Cowan C, Pouladi MA, Metzler M, Bissada N, Wang L, Faull RL, Gray M, Yang XW, Raymond LA, Hayden MR. Cleavage at the 586 amino acid caspase-6 site in mutant huntingtin influences caspase-6 activation in vivo. J Neurosci. 2010; 30:15019–15029. [PubMed: 21068307]

Graham RK, Deng Y, Slow EJ, Haigh B, Bissada N, Lu G, Pearson J, Shehadeh J, Bertram L, Murphy Z, Warby SC, Doty CN, Roy S, Wellington CL, Leavitt BR, Raymond LA, Nicholson DW, Hayden MR. Cleavage at the caspase-6 site is required for neuronal dysfunction and degeneration due to mutant huntingtin. Cell. 2006; 125:1179–1191. [PubMed: 16777606]

Gray M, Shirasaki DI, Cepeda C, Andre VM, Wilburn B, Lu XH, Tao J, Yamazaki I, Li SH, Sun YE, Li XJ, Levine MS, Yang XW. Full-length human mutant huntingtin with a stable polyglutamine repeat can elicit progressive and selective neuropathogenesis in BACHD mice. J Neurosci. 2008; 28:6182–6195. [PubMed: 18550760]

Guo H, Albrecht S, Bourdeau M, Petzke T, Bergeron C, LeBlanc AC. Active caspase-6 and caspase-6-cleaved tau in neuropil threads, neuritic plaques, and neurofibrillary tangles of Alzheimer's disease. The American journal of pathology. 2004; 165:523–531. [PubMed: 15277226]

Gutekunst C-A, Li S-H, Yi H, Mulroy JS, Kuemmerle S, Jones R, Rye D, Ferrante RJ, Hersch SM, Li X-J. Nuclear and neuropil aggregates in Huntington's disease: relationship to neuropathology. Journal of Neuroscience. 1999; 19:2522–2534. [PubMed: 10087066]

HDCRG. A novel gene containing a trinucleotide repeat that is expanded and unstable on Huntington's disease chromosomes. The Huntington's Disease Collaborative Research Group. Cell. 1993; 72:971–983. [PubMed: 8458085]

Hermel E, Gafni J, Propp SS, Leavitt BR, Wellington CL, Young JE, Hackam AS, Logvinova AV, Peel AL, Chen SF, Hook V, Singaraja R, Krajewski S, Goldsmith PC, Ellerby HM, Hayden MR, Bredesen DE, Ellerby LM. Specific caspase interactions and amplification are involved in selective neuronal vulnerability in Huntington's disease. Cell Death Differ. 2004; 11:424–438. [PubMed: 14713958]

Hodgson JG, Agopyan N, Gutekunst CA, Leavitt BR, LePiane F, Singaraja R, Smith DJ, Bissada N, McCutcheon K, Nasir J, Jamot L, Li XJ, Stevens ME, Rosemond E, Roder JC, Phillips AG, Rubin EM, Hersch SM, Hayden MR. A YAC mouse model for Huntington's disease with full-length mutant huntingtin, cytoplasmic toxicity, and selective striatal neurodegeneration. Neuron. 1999; 23:181–192. [PubMed: 10402204]

Hoffner G, Soues S, Djian P. Aggregation of expanded huntingtin in the brains of patients with Huntington disease. Prion. 2007; 1:26–31. [PubMed: 19172113]

Jeong H, Then F, Melia TJ Jr, Mazzulli JR, Cui L, Savas JN, Voisine C, Paganetti P, Tanese N, Hart AC, Yamamoto A, Krainc D. Acetylation targets mutant huntingtin to autophagosomes for degradation. Cell. 2009; 137:60–72. [PubMed: 19345187]

Kegel KB, Sapp E, Alexander J, Reeves P, Bleckmann D, Sobin L, Masso N, Valencia A, Jeong H, Krainc D, Palacino J, Curtis D, Kuhn R, Betschart C, Sena-Esteves M, Aronin N, Paganetti P, Difiglia M. Huntingtin cleavage product A forms in neurons and is reduced by gamma-secretase inhibitors. Molecular neurodegeneration. 2010; 5:58. [PubMed: 21156064]

Lee ST, Kim M. Aging and neurodegeneration. Molecular mechanisms of neuronal loss in Huntington's disease. Mechanisms of ageing and development. 2006; 127:432–435. [PubMed: 16527334]

Leyva MJ, Degiacomo F, Kaltenbach LS, Holcomb J, Zhang N, Gafni J, Park H, Lo DC, Salvesen GS, Ellerby LM, Ellman JA. Identification and evaluation of small molecule pan-caspase inhibitors in Huntington's disease models. Chem Biol. 2010; 17:1189–1200. [PubMed: 21095569]

Lin CH, Tallaksen-Greene S, Chien WM, Cearley JA, Jackson WS, Crouse AB, Ren S, Li XJ, Albin RL, Detloff PJ. Neurological abnormalities in a knock-in mouse model of Huntington's disease. Hum Mol Genet. 2001; 10:137–144. [PubMed: 11152661]

Lunkes A, Lindenberg KS, Ben-Haiem L, Weber C, Devys D, Landwehrmeyer GB, Mandel JL, Trottier Y. Proteases acting on mutant huntingtin generate cleaved products that differentially build up cytoplasmic and nuclear inclusions. Molecular cell. 2002; 10:259–269. [PubMed: 12191472]

MacFarlane M. Compensatory caspase activation: a cautionary tale. Trends in pharmacological sciences. 2001; 22:60. [PubMed: 11166841]

Martindale D, Hackam A, Wieczorek A, Ellerby L, Wellington C, McCutcheon K, Singaraja R, Kazemi-Esfarjani P, Devon R, Kim SU, Bredesen DE, Tufaro F, Hayden MR. Length of huntingtin and its polyglutamine tract influences localization and frequency of intracellular aggregates. Nat Genet. 1998; 18:150–154. [PubMed: 9462744]

McStay GP, Salvesen GS, Green DR. Overlapping cleavage motif selectivity of caspases: implications for analysis of apoptotic pathways. Cell Death Differ. 2008; 15:322–331. [PubMed: 17975551]

Menalled L, El-Khodor BF, Patry M, Suarez-Farinas M, Orenstein SJ, Zahasky B, Leahy C, Wheeler V, Yang XW, MacDonald M, Morton AJ, Bates G, Leeds J, Park L, Howland D, Signer E, Tobin A, Brunner D. Systematic behavioral evaluation of Huntington's disease transgenic and knock-in mouse models. Neurobiol Dis. 2009; 35:319–336. [PubMed: 19464370]

Nikolaev A, McLaughlin T, O'Leary DD, Tessier-Lavigne M. APP binds DR6 to trigger axon pruning and neuron death via distinct caspases. Nature. 2009; 457:981–989. [PubMed: 19225519]

Norman JM, Cohen GM, Bampton ET. The in vitro cleavage of the hAtg proteins by cell death proteases. Autophagy. 2010; 6:1042–1056. [PubMed: 21121091]

Ravikumar B, Duden R, Rubinsztein DC. Aggregate-prone proteins with polyglutamine and polyalanine expansions are degraded by autophagy. Hum Mol Genet. 2002; 11:1107–1117. [PubMed: 11978769]

Ravikumar B, Vacher C, Berger Z, Davies JE, Luo S, Oroz LG, Scaravilli F, Easton DF, Duden R, O'Kane CJ, Rubinsztein DC. Inhibition of mTOR induces autophagy and reduces toxicity of polyglutamine expansions in fly and mouse models of Huntington disease. Nat Genet. 2004; 36:585–595. [PubMed: 15146184]

Richards P, Didszun C, Campesan S, Simpson A, Horley B, Young KW, Glynn P, Cain K, Kyriacou CP, Giorgini F, Nicotera P. Dendritic spine loss and neurodegeneration is rescued by Rab11 in models of Huntington's disease. Cell Death Differ. 2011; 18:191–200. [PubMed: 21217767]

Sanchez I, Mahlke C, Yuan J. Pivotal role of oligomerization in expanded polyglutamine neurodegenerative disorders. Nature. 2003; 421:373–379. [PubMed: 12540902]

Singer J. Using SAS PROC MIXED to Fit Multilevel Models, Hierarchical Models, and Individual Growth Models. Journal of Educational and Behavioral Statistics. 1998; 23:323.

Sivananthan SN, Lee AW, Goodyer CG, LeBlanc AC. Familial amyloid precursor protein mutants cause caspase-6-dependent but amyloid beta-peptide-independent neuronal degeneration in primary human neuron cultures. Cell death & disease. 2010; 1:e100. [PubMed: 21368865]

Steffan JS, Kazantsev A, Spasic-Boskovic O, Greenwald M, Zhu YZ, Gohler H, Wanker EE, Bates GP, Housman DE, Thompson LM. The Huntington's disease protein interacts with p53 and CREB-binding protein and represses transcription. Proceedings of the National Academy of Sciences of the United States of America. 2000; 97:6763–6768. [PubMed: 10823891]

Uribe V, et al. Rescue from excitotoxicity and axonal degeneration accompanied by age-dependent behavioral and neuroanatomical alterations in caspase-6-deficient mice. Hum Mol Genet. 2012

Van Raamsdonk JM, Gibson WT, Pearson J, Murphy Z, Lu G, Leavitt BR, Hayden MR. Body weight is modulated by levels of full-length huntingtin. Hum Mol Genet. 2006; 15:1513–1523. [PubMed: 16571604]

Wellington CL, Singaraja R, Ellerby L, Savill J, Roy S, Leavitt B, Cattaneo E, Hackam A, Sharp A, Thornberry N, Nicholson DW, Bredesen DE, Hayden MR. Inhibiting caspase cleavage of huntingtin reduces toxicity and aggregate formation in neuronal and nonneuronal cells. Journal of Biological Chemistry. 2000; 275:19831–19838. [PubMed: 10770929]

Wellington CL, Ellerby LM, Gutekunst CA, Rogers D, Warby S, Graham RK, Loubser O, van Raamsdonk J, Singaraja R, Yang YZ, Gafni J, Bredesen D, Hersch SM, Leavitt BR, Roy S, Nicholson DW, Hayden MR. Caspase cleavage of mutant huntingtin precedes neurodegeneration in Huntington's disease. J Neurosci. 2002; 22:7862–7872. [PubMed: 12223539]

Wellington CL, et al. Caspase cleavage of gene products associated with triplet expansion disorders generates truncated fragments containing the polyglutamine tract. The Journal of biological chemistry. 1998; 273:9158–9167. [PubMed: 9535906]

Zhang H, Li Q, Graham RK, Slow E, Hayden MR, Bezprozvanny I. Full length mutant huntingtin is required for altered Ca2+ signaling and apoptosis of striatal neurons in the YAC mouse model of Huntington's disease. Neurobiol Dis. 2008; 31:80–88. [PubMed: 18502655]

Zheng TS, Hunot S, Kuida K, Momoi T, Srinivasan A, Nicholson DW, Lazebnik Y, Flavell RA. Deficiency in caspase-9 or caspase-3 induces compensatory caspase activation. Nature medicine. 2000; 6:1241–1247.

Zois CE, Giatromanolaki A, Sivridis E, Papaiakovou M, Kainulainen H, Koukourakis MI. "Autophagic flux" in normal mouse tissues: Focus on endogenous LC3A processing. Autophagy. 2011; 7

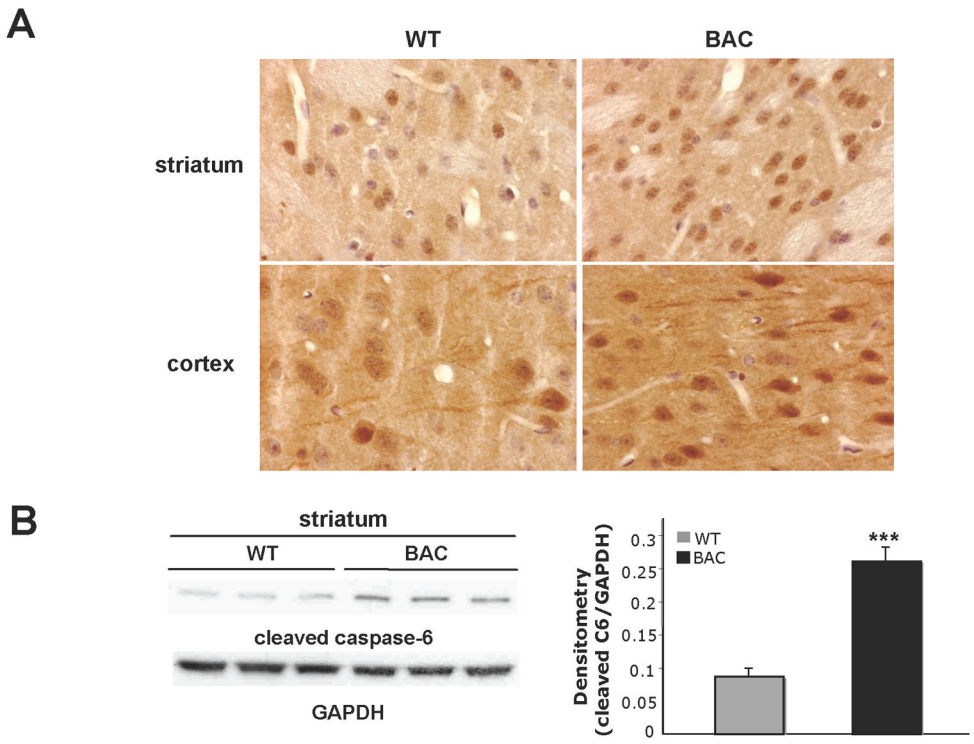

Figure 1. Cleaved caspase-6 is increased in BACHD mice

(A) Immunohistochemistry of cleaved caspase-6 in 9-month old WT and BACHD striatum and cortex. Tissue is counterstained with hematoxylin. (B) Western blot of cleaved caspase-6 levels in 9-month old WT and BACHD striatum (left panel). Densitometry of cleaved caspase-6 normalized to GAPDH (right panel; n=3, t-test, ***, $p<0.001$).

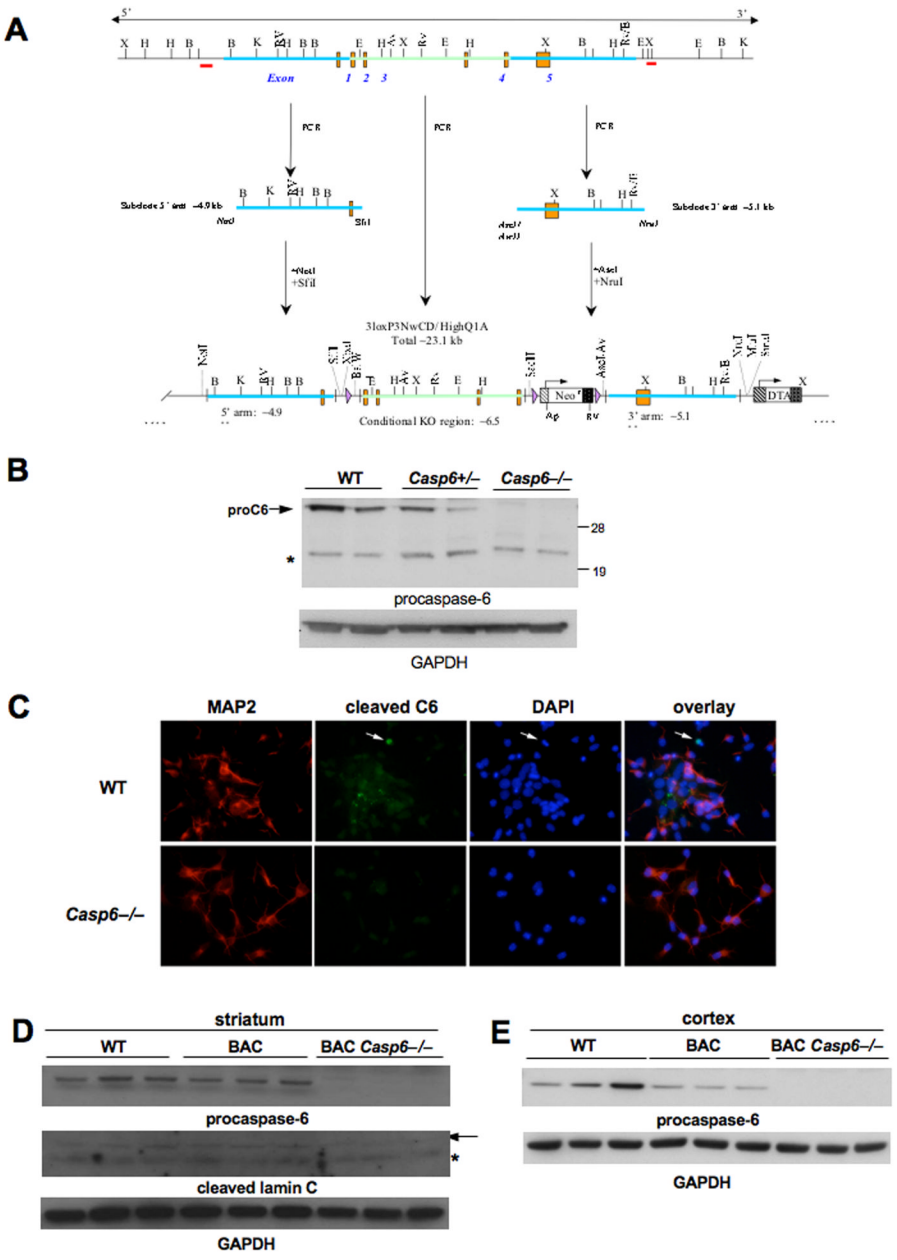

Figure 2. Knocking out capase-6 eliminates caspase-6 expression

(A) Vector scheme for caspase-6 knockout mouse. (B) Western blot of procaspase-6 protein in 15-month old WT, *Casp6+/–*and *−/−* cortex. Band to right of asterisk is non-specific. (C) Immunocytochemistry of cleaved caspase-6 in WT and *Casp6−/−* striatal neuronal cultures. (D) Western blot of procaspase-6 and cleaved lamin C protein production in 13-month old WT, BACHD and BACHD *Casp6−/−* striatal lysates. Arrow points to cleaved lamin C and asterisk indicates nonspecific band. (E) Western blot of procaspase-6 levels in 13-month old WT, BACHD and BACHD *Casp6−/−* cortical lysates.

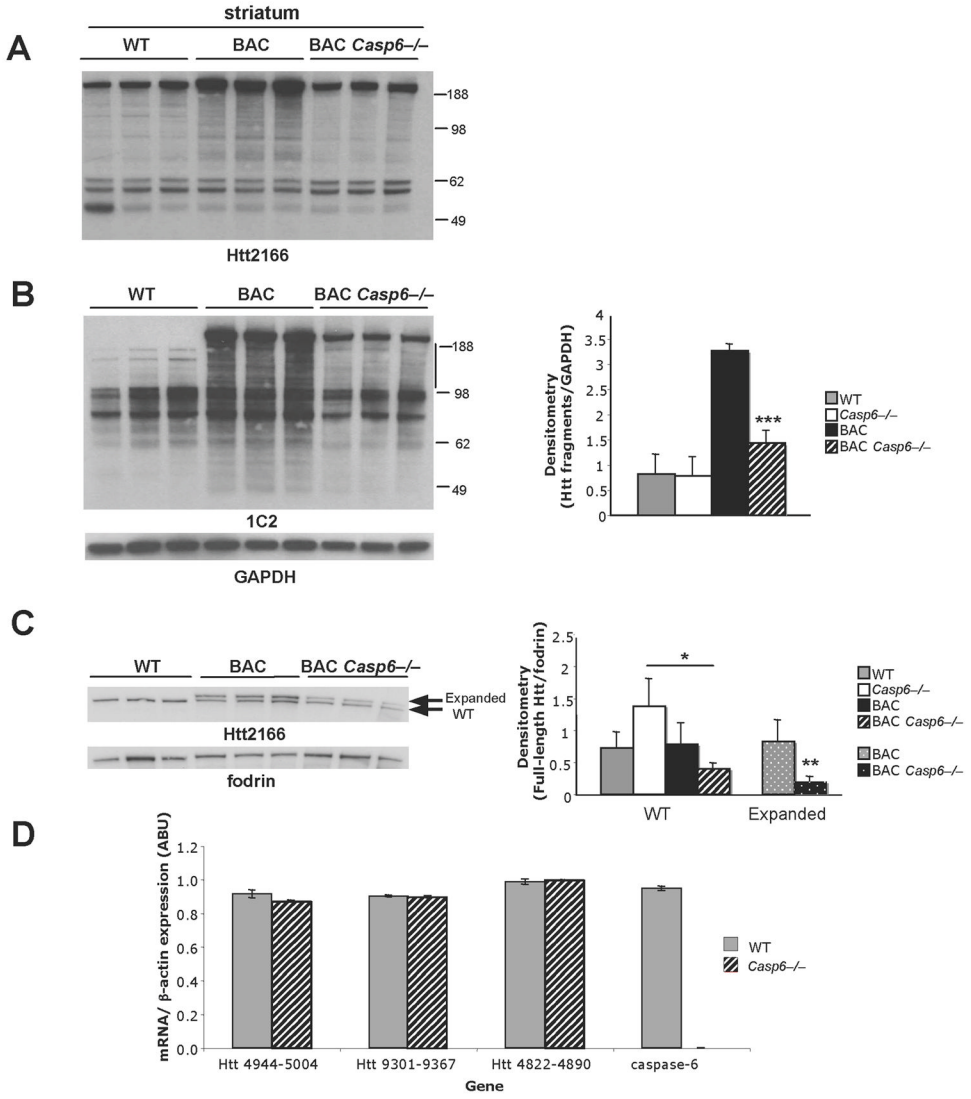

Figure 3. Full-length Htt and Htt fragments are reduced in BACHD *Casp6*−/−striatal lysates

(A) Western blot of striatal lysates from 13-month old animals probed with Htt2166 antibody, an antibody that detects both wild-type and expanded Htt. (B) Western blot of 13-month old striatal lysates probed with an antibody that preferentially detects expanded Htt (1C2) (left panel). Densitometry of Htt fragments between 98 and 188 kDa in left panel (left of line) normalized to GAPDH (right panel; n=3, ANOVA, ***, p<0.001). (C) Further separation of full-length wild-type and expanded striatal Htt visualized with Htt2166 antibody using western blot analysis (left panel). Densitometry of full-length expanded Htt relative to wild-type Htt from left panel (right panel; n=3, WT, ANOVA *, p <0.05; Expanded, t-test, **, p <0.01). (D) Quantitative RT-PCR of Htt and caspase-6 in 12-month old WT and *Casp6*−/− striatum. Numbers on x-axis indicates region of nucleotide amplification.

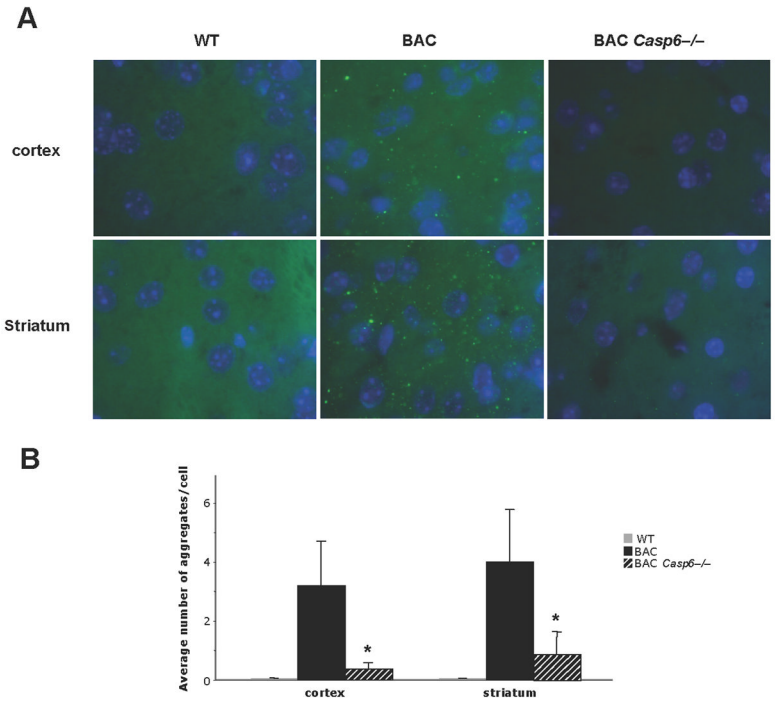

Figure 4. Aggregate formation is reduced in BACHD *Casp6*−/−striatum and cortex

(A) Immunofluorescence of 13-month old cortex and striatum using the S830 Htt aggregate antibody counterstained with DAPI. (B) Quantification of aggregates shows a dramatic decrease in number in BACHD *Casp6*−/− (n=3–6, ANOVA, *, p <0.05).

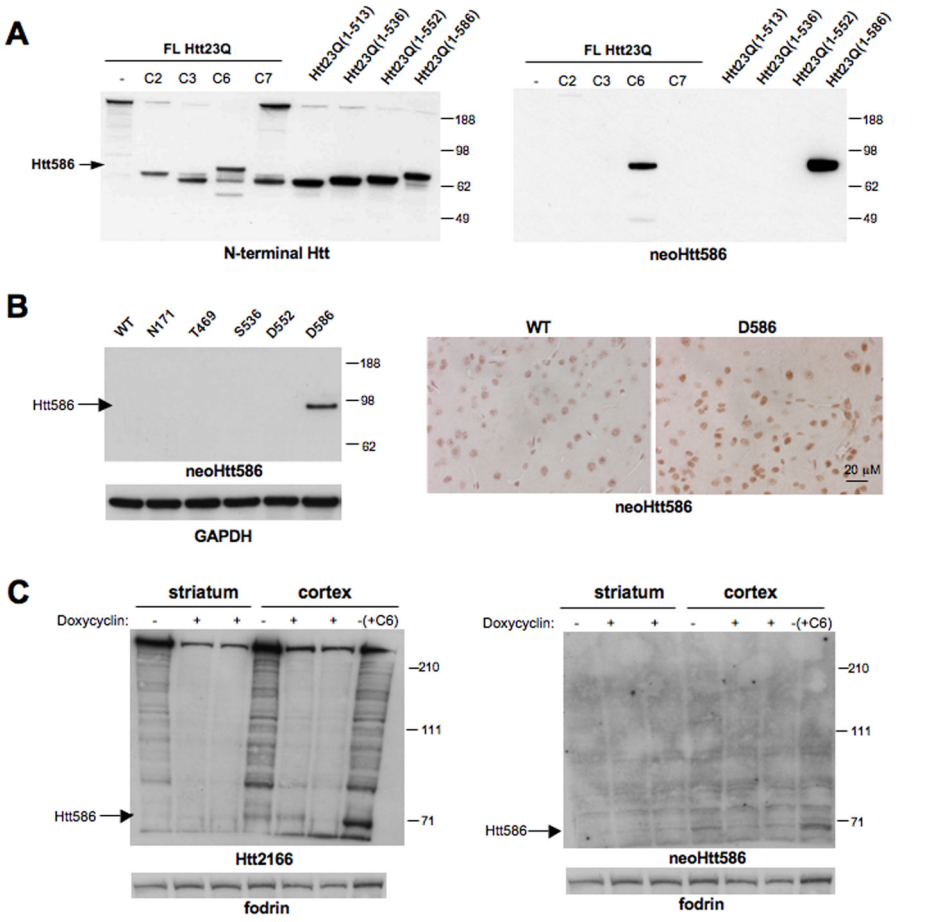

Figure 5. NeoHtt586 antibody is specific for the caspase-6 cleaved product of Htt

(A) Lysates from 293T cells over-expressing full-length Htt 23Q treated with caspase-2, caspase-3, caspase-6 and caspase-7 and Htt23Q(1–513), Htt23Q(1–536), Htt23Q(1–552) and Htt23Q(1–586) were used to verify neoHtt586 specificity. Western blots were probed with an N-terminal Htt antibody (left panel) and a neoHtt586 antibody (right panel). (B) Western blot of cortical lysates from WT mice and mice expressing expanded Htt constructs with 171, 469, 536, 552, and 586 amino acids probed with noeHtt586 antibody (left panel). NeoHtt586 immunohistochemistry of WT and D586 cortex (right panel). (C) Cortical and striatal lysates from Htt knockdown mice with and without doxycyclin treatment analyzed by western blot. Control cortical lysates were treated with recombinant caspase-6 as a positive control (+C6). Samples were probed with a Htt antibody (left panel) and an antibody that specifically interacts with the caspase-6 produced Htt fragment (neoHtt586) (right panel). Fodrin was used as a loading control.

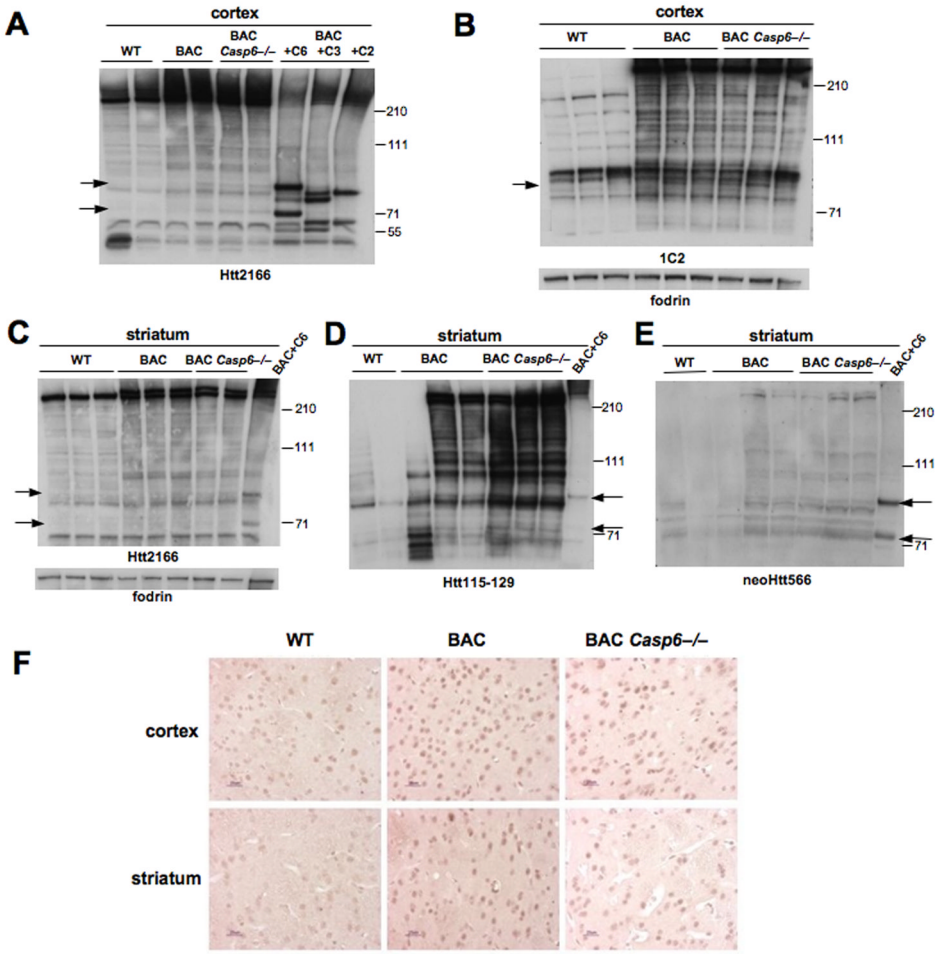

Figure 6. Fragments similar in size to Htt586 are present in BACHD *Casp6*−/−cortex and striatum

(A) Western blot of cortical lysates from 13-month old animals with caspase-6, caspase-3 and caspase-2 treated lysates probed with Htt2166 antibody. Arrows indicate Htt586 products. (B) Western blot of 13-month old cortical lysates probed with 1C2 antibody. Fodrin shows equal loading. Arrow indicates size of expanded Htt586. (C) Western blot of 15-month old striatal lysates probed with Htt2166 antibody. Fodrin shows equal loading. Arrows indicate size of Htt586 products. (D) N-terminal Htt antibody (Htt115–129) detects Htt586 fragments in 13-month old solubilized striatal pellet western blot. Arrows indicate size of Htt586 products. (E) A neoHtt586 antibody detects Htt586 fragments in 13-month old solubilized striatal pellets. Arrows indicate size of Htt586 products. (F) Immunohistochemistry with a neoHtt586 antibody in 15-month old cortex and striatum shows an increase in staining in BACHD and a subsequent decrease in staining in BACHD *Casp6*−/− most likely reflecting lower Htt levels overall.

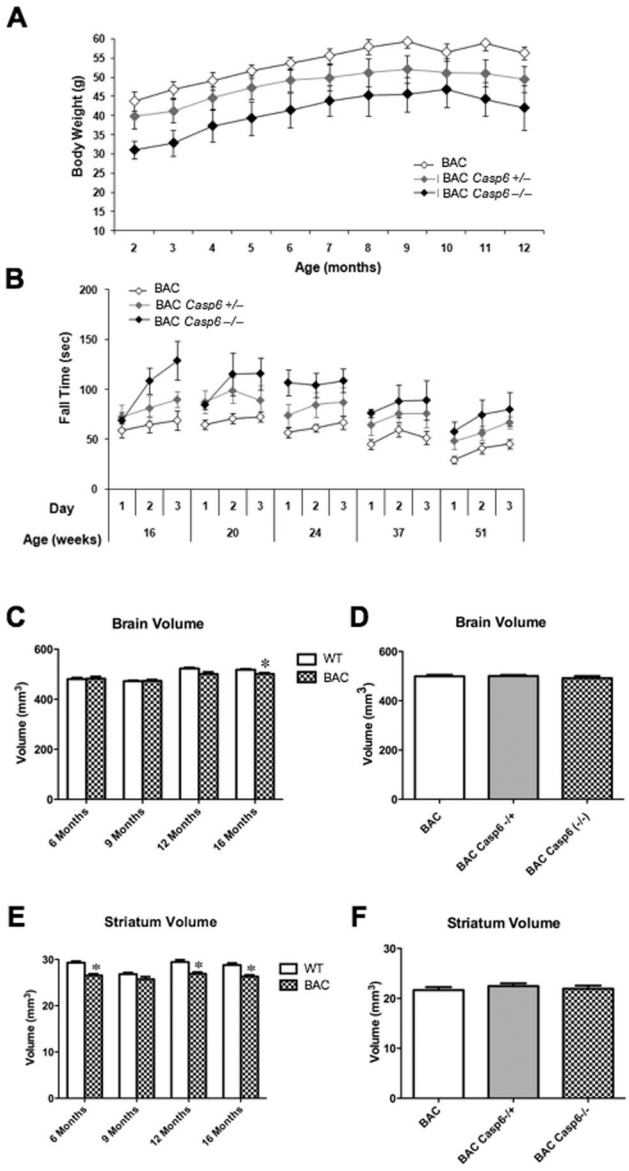

Figure 7. Effect of caspase-6 deletion on development and behavior

(A) Knockout of caspase-6 produced a significant reduction in body weight of BACHD mice when compared to WT animals (*ps* <0.05) (B) Deletion of caspase-6 improves rotarod performance in the BACHD mice (*ps* <0.05). See Data Analysis for Weight and Behavior in Material and Methods for statistical analysis. (C) BACHD mice had significantly smaller whole brain volume at 16 months of age (t-test, *, p<0.05, compared to WT mice). (E) BACHD mice had significantly smaller striatal volumes at 6, 12 and 16 months of age (t-test, *, p<0.05, compared to WT mice). (D, F) Brain and striatal volumes were unaffected in BACHD *Casp6+/−*and BACHD *Casp6−/−* mice relative to BACHD.

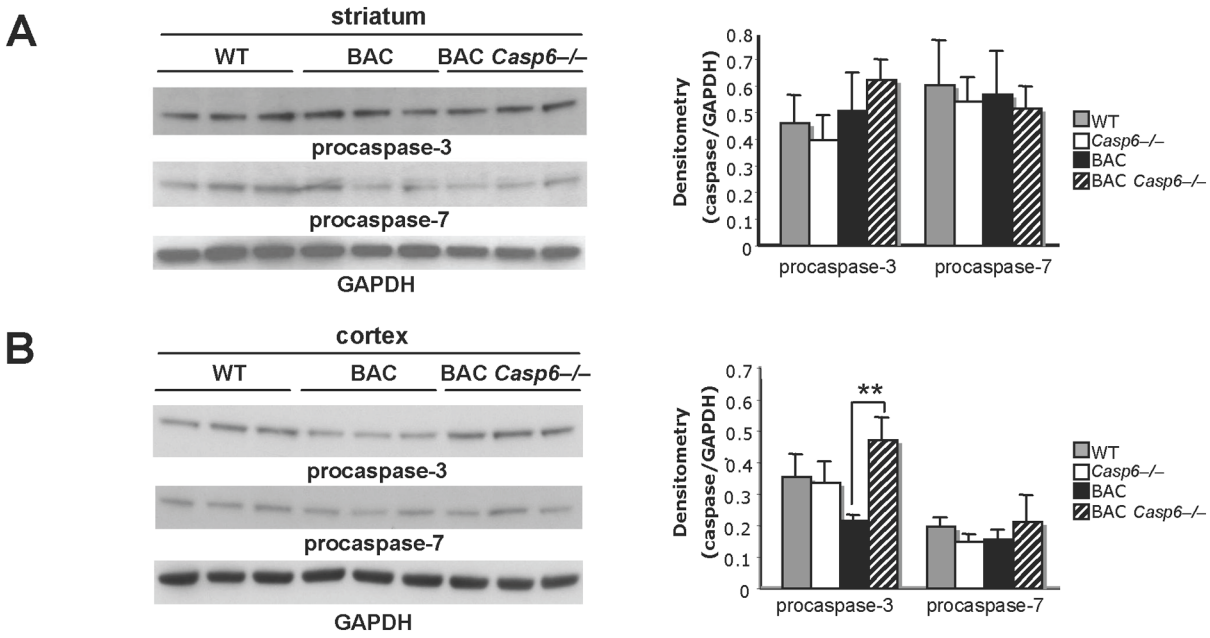

Figure 8. Compensatory changes in caspase levels are modest in BAC *Casp6*−/−mice

(A) Western blot of procaspase-3 and procaspase-7 protein levels in 13-month old striatum (left panel). Densitometry of striatal caspases normalized to GAPDH (right panel). (B) Western blot of procaspase-3 and procaspase-7 protein levels in 13-month old cortex (left panel). Densitometry of cortical caspases normalized to GAPDH (right panel; n=3, ANOVA, **, $p<0.01$).

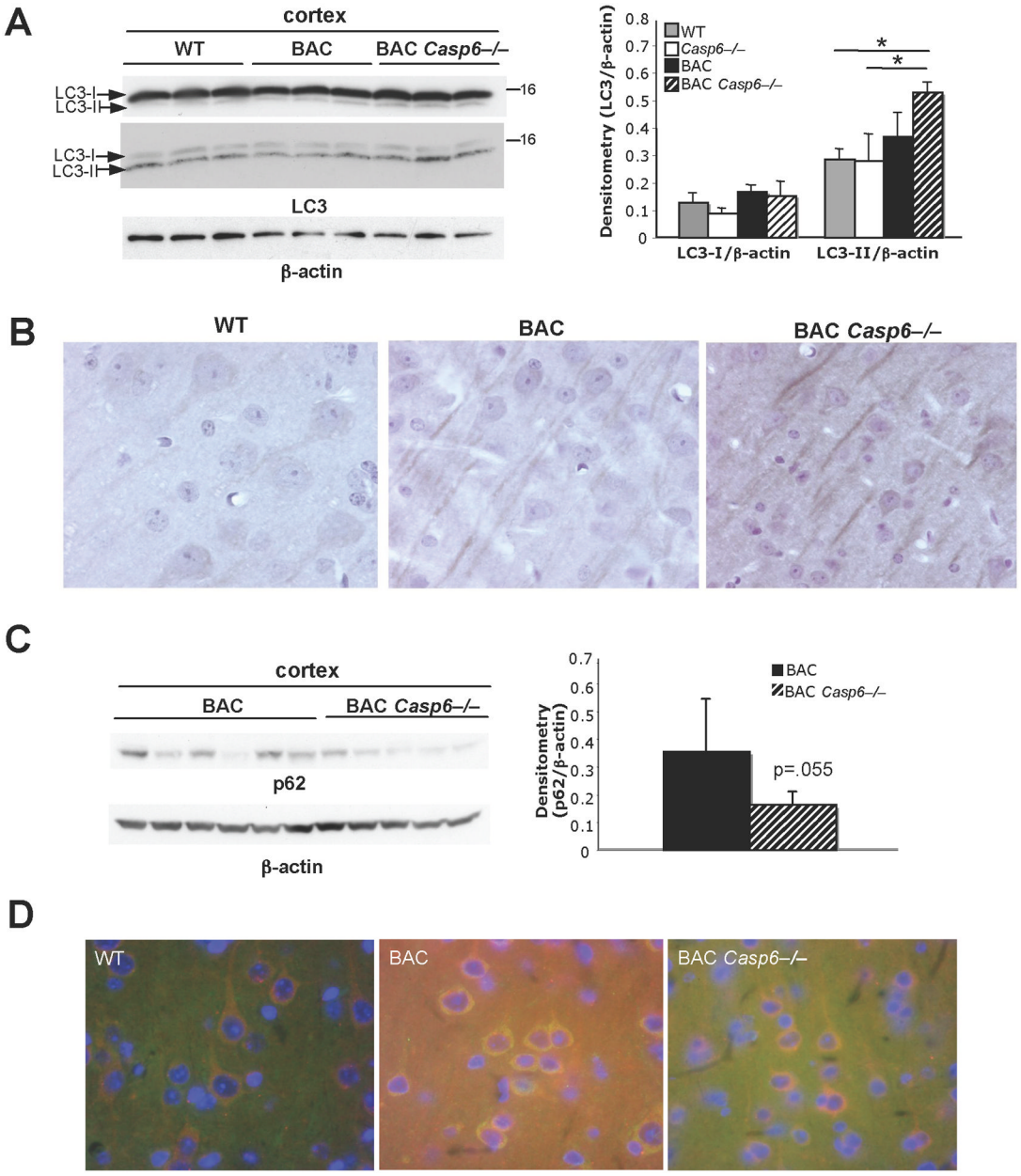

Figure 9. Autophagy-associated proteins are altered in 13-month old BACHD*Casp6*−/− mice

(A) Western analysis shows an increase in LC3-II levels in BACHD *Casp6*−/− cortex with antibodies from MBL (top left panel) and Abgent (middle left panel). Densitometry of cortical LC3 levels (Abgent antibody) normalized to β-actin (right panel; n=3, ANOVA *, p< 0.05). (B) Immunohistochemistry shows an increase in LC3 immunoreactivity and altered localization in the 13-month old BACHD *Casp6*−/− cortex relative to both WT and BACHD. (C) p62 protein levels decrease in BACHD *Casp6*−/− cortex relative to BACHD (left panel; 13- and 15-month old cortex) using western blot analysis. Densitometry of p62 normalized to β-actin (right panel; n=5–6, t-test). (D) Immunohistochemistry shows co-localization of p62 (red) and Htt acetylated at aa K444 (green) in 13-month old cortex.

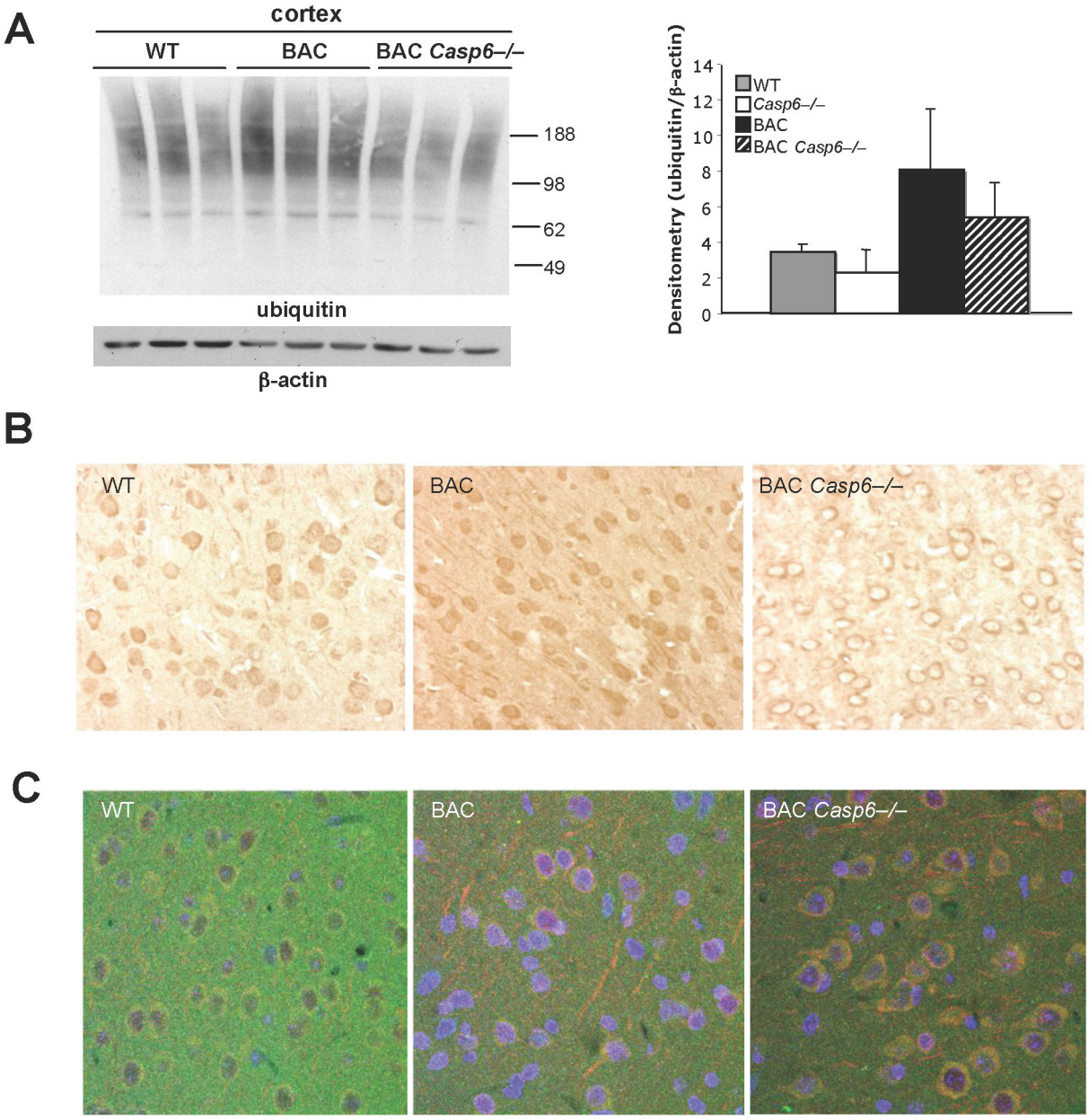

Figure 10. Ubiquitination levels increase in BACHD and BACHD *Casp6*−/− mice

(A) Western analysis shows an increase in overall protein ubiquitination levels in 13-month old cortex (left panel). Densitometry of total ubiquitinated protein normalized to β-actin (right panel; n=3). (B) Immunohistochemistry shows changes in localization of ubiquitinated proteins in 15-month old BACHD *Casp6*−/− cortex. (C) Double immunofluorescence of ubiquitin (red) and huntingtin (green) confirms co-localization in 13-month old cortex. DAPI nuclear stain is in blue.